Ab-Initio Anharmonic Analysis of Complex Vibrational Spectra of Phenylacetylene and Fluorophenylacetylenes in the Acetylenic and Aromatic C–H Stretching Region

Sumitra Singh,[1] Qian-Rui Huang,[2] Jake A. Tan,[2] Jer-Lai Kuo,*[2] and G. Naresh Patwari*[1]

[1] Department of Chemistry, Indian Institute of Technology Bombay, Powai, Mumbai 400076 India. E-mail: naresh@chem.iitb.ac.in

[2] Institute of Atomic and Molecular Sciences, Academia Sinica, Taipei 10617, Taiwan. E-mail: jlkuo@pub.iams.sinica.edu.tw

ABSTRACT

Vibrational spectra in the acetylenic and aromatic C–H stretching region of phenylacetylene and fluorophenylacetylenes viz., 2-fluorophenylacetylene, 3-fluorophenylacetylene and 4-fluorophenylacetylene, were measured using IR-UV double resonance spectroscopic method. The spectra, in both acetylenic and aromatic C–H stretching regions, were complex exhibiting multiple bands. *Ab-initio* anharmonic calculations with quartic potential (QP) using B97D3/6-311++G(d,p) and vibrational configuration interaction (VCI) were able to capture all important spectral features, in both the regions of the experimentally observed spectra for all four molecules considered in the present work. Interestingly, for phenylacetylene, the spectrum in the acetylenic C–H stretching region emerges due to anharmonic coupling of mode localized on the acetylenic moiety along with the other ring modes which also involve displacements on the acetylenic group, which is in contrast to what has been proposed and propagated in the literature. In general, this coupling scheme is invariant to the fluorine atom substitution. For the aromatic C–H stretching region the observed spectrum emerges due to the coupling of the C–H stretching with C–C stretching and C–H in-plane bending modes.
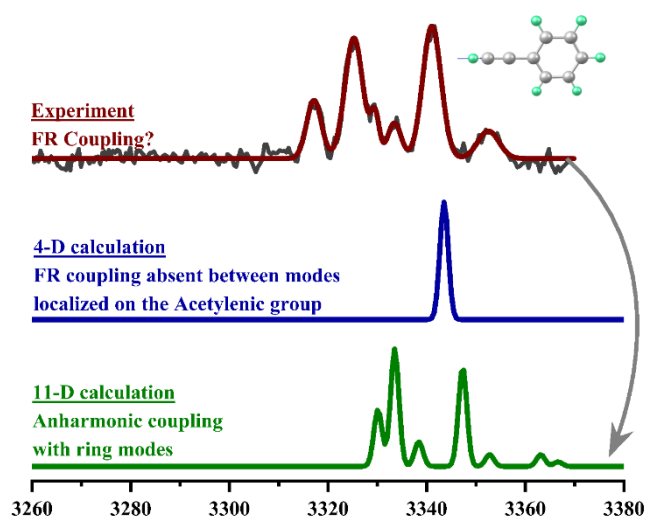
INTRODUCTION

Infrared spectroscopy of the X–H groups has long been used as a spectroscopic tool to investigate the intermolecular interactions, as the IR spectra of the X–H stretching vibration show characteristic frequency shifts which can be related to the intermolecular structures.[1,2] However, in some instances the IR spectra of the X–H stretching vibration, especially the spectra corresponding to the C–H and the N–H oscillators are complicated due to anharmonic coupling.[3,4] For instance, the IR spectrum in the acetylenic C–H stretching region of phenylacetylene (PHA) shows two strong bands accompanied by several weaker bands. In this case, the two strong transitions have been assigned to arise from Fermi resonance coupling between the acetylenic C–H stretching vibration with the combination mode of one quantum of the C≡C stretching mode and two quanta of the C≡C–H out-of-plane bending mode, based on the comparative study of infrared spectra of various molecules containing the acetylenic groups.[5–7] On the other hand, several weaker bands have been attributed to the higher order couplings which gain intensity due to "partial saturation inherent to depletion spectroscopy",[7] which is one of the techniques used to record the IR spectra. The spectra in the acetylenic C–H stretching region have been interpreted to arrive at the intermolecular structures of several hydrogen-bonded and π-stacked structures of phenylacetylene.[8,9] Similarly in the case of fluorophenylacetylenes, once again, the IR spectra in the acetylenic C–H stretching region also show multiple bands due to anharmonic coupling, and once again have been interpreted to understand various intermolecular structures.[10,11] Further, the intermolecular interactions present in gas phase clusters of phenylacetylene[12] and fluorophenylacetylenes[13] up to four monomeric units have also been investigated, and the IR spectral features in the acetylenic C–H stretching region of the clusters are very similar to the corresponding monomers. On the other hand, the spectral features in the aromatic C–H stretching region were marginally different than the corresponding monomers, based on the extent of their involvement in the intermolecular interactions in gas-phase clusters. Similarly, in the case of methylamine and its clusters, the IR spectra in the alkyl C–H stretching region also show complicated features due to anharmonic coupling.[14] Moreover, complex IR spectra have been used as an important spectroscopic probe to distinguish and determine conformations of various complex molecular systems.[15,16]

Theoretical attempts to comprehend the intricate spectral features resulting from Fermi resonance and other anharmonic coupling have been put forth in the past decade.[16–25] However, the theoretical treatment of Fermi resonance coupling in acetylenic C–H stretching region are sparse. An effective computational approach based on the ab-initio method for the treatment of FR coupling is the use of the quartic potential-vibrational configurational interaction (QP-VCI) method, wherein all the cubic and part of the quartic terms are included in the potential energy surface (PES) operator and the corresponding eigenvalue problem is solved by the vibrational configurational interaction (VCI) method.[17,26] In this work, vibrational spectra of phenylacetylene (PHA) and singly fluorine substituted phenylacetylenes, 2-fluorophenylacetylne (2FPHA), 3-fluorophenylacetylne (3FPHA) and 4-fluorophenylacetylne (4FPHA), depicted in Figure 1, in the acetylenic C–H ({Ac}C–H) stretching region is investigated using ab-initio anharmonic QP-VCI method and compared with the experimentally observed spectra. Further, the vibrational spectra in the aromatic C–H ({Ar}C–H) are also calculated.
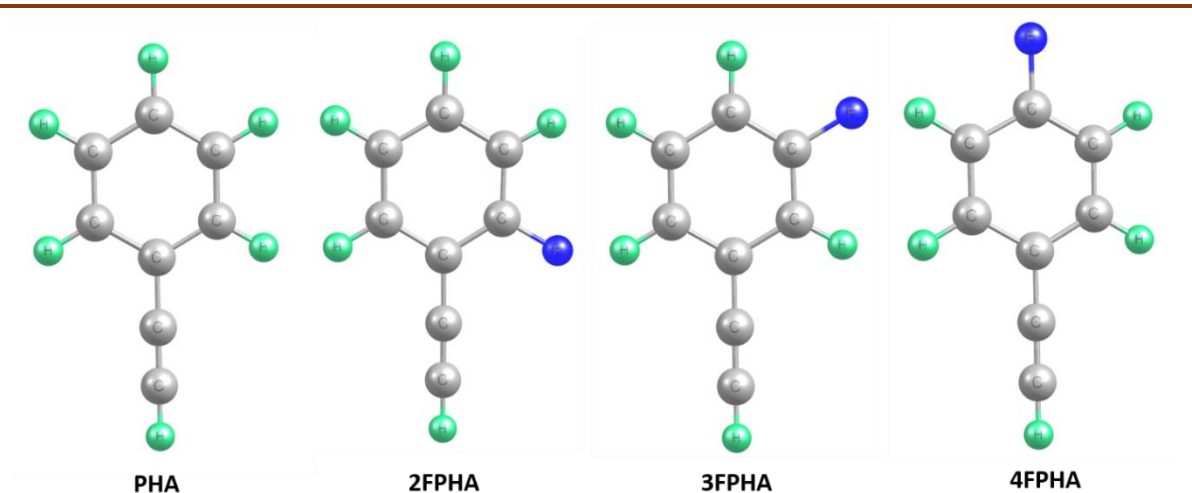

Figure 1. Structures of phenylacetylene and fluorophenylacetylenes considered in the present work.

METHODOLOGY

The IR spectra of phenylacetylene and fluorophenylacetylenes in the acetylenic and aromatic C–H stretching region were recorded using the fluorescence dip infrared (FDIR) spectroscopic method.[27,28] For this purpose, a seeded supersonic free-jet was produced by the co-expansion of desired reagents in helium buffer gas held at high pressure

(typically 2 atm) through a 500μm diameter pulsed nozzle (series 9; General Valve Corporation), driven by a pulsed valve driver (Iota One; General Valve Corporation) into a high vacuum chamber. The supersonically expanded molecules were excited by a UV laser and the ensuing fluorescence was detected using a PMT (Photomultiplier tube)/filter (WG305) combination.[29] For recording the FDIR spectrum, an IR laser was introduced 100 ns prior to the UV laser, and the depletion in the population of the ground state induced by resonant vibrational transition lowers the fluorescence signal due to the UV laser. This depletion in the fluorescence signal as a function of IR laser frequency yields the FDIR spectrum. In the present set of experiments, the tunable UV laser is a frequency-doubled output of a dye laser (Narrow scan GR; Radiant Dyes) pumped by the second harmonic of a Q-switched Nd:YAG laser (Brilliant B; Quantel) and the tunable IR laser is an idler component of an optical parametric oscillator (custom LiNbO3 OPO; Euroscan Instruments) pumped with the fundamental (1064 nm) of an injection seeded Nd:YAG laser (Brilliant B: Quantel). The typical bandwidth of both UV and IR lasers is about1 cm^{-1}, and the absolute frequency calibration is within ±2 cm^{-1}. In a typical experiment the power of the UV and IR pulses are about 100 μJ and 2 mJ, respectively. Further, the timing of the opening of the pulse valve, and the firing of the IR and UV laser pulses is controlled by a Digital Delay Generator (555-4C; Berkley Nucleonics Corporation).

To compare with experimental spectra in the {Ac}C–H and {Ar}C–H stretching regions, the structures of the four monomers, PHA, 2FPHA, 3FPHA and 4FPHA, were optimized at B97D3/6-311++G(d,p) level using Gaussian 16 suit of programs.[30] Normal modes were evaluated from the Hessian matrix at the same level as the starting point for the theoretical treatment. Quartic potential (QP) was constructed from the Hessian matrices evaluated at the same DFT level with a finite difference method from minima along the normal modes selected. Instead of using second-order vibrational perturbation theory,[31] the approximate vibrational Hamiltonian was constructed using the direct product of either harmonic wavefunctions or eigenfunctions of one-dimensional QP as basis sets. Direct diagonalization of the vibrational Hamiltonian, known as vibrational configuration interaction (VCI), was used to solve eigenvalue problems. The details of our implementations of QP+VCI can be found elsewhere,[25] and only a brief summary is provided here. In this work, QP along selected normal modes and VCI including 4 body interactions and up to 5 quanta excitation in the modes were considered for the spectral

simulations. The assignment is based on projecting the final eigenfunction to the solution of one-dimensional solutions with QP. Even with the above-mentioned setting, the application of our VCI implementation is limited to about 25 dimensions when many low-frequency (< 1000 cm^{-1}) modes were included.[32] The IR spectra in the {Ac}C–H stretching regions considered eleven modes in the simulation for all the monomers, which includes some ring modes that have displacements of the C–C≡C moiety along with C≡C and {Ac}C–H stretching and {Ac}C–H bending modes (see the supporting information). On the other hand, the spectral simulation in the {Ar}C–H stretching region includes all the aromatic C–H stretching modes along with all the C–C stretching and in-plane aromatic C–H bending modes greater than 1000 cm^{-1} (see the supporting information).

RESULTS AND DISCUSSION

The FDIR spectra of the PHA, 4FPHA, 2FPHA, and 3FPHA monomers in the {Ac}C–H stretching region are shown in Figure 2. Complex spectral features consisting of multiple bands were observed for PHA, which is indicative of the presence of higher-order anharmonic coupling among the different vibrational modes of the system. Comparison of the experimental IR spectra in the {Ac}C–H regions suggests the similarity between the PHA and 4FPHA spectra, which can be rationalized based on the symmetry of the molecule (C_{2v}). In the case of PHA (Figure 2I), the two intense bands at 3325 (**b**) and 3341 cm^{-1} (**e**) were attributed to be arising out of Fermi resonance coupling between the {Ac}C–H stretch and the combination band arising out of one quantum of C≡C stretch and two quanta of C≡C-H out-of-plane bend,[6,7] while the weaker bands at 3317 (**a**), 3330 (**c**), 3333 (**d**), and 3353 (**f**) cm^{-1} are originating from other higher-order couplings.[33] This essentially implies that the Fermi resonance coupling in PHA is localized on the acetylenic moiety. However, considering only the four fundamental modes localized on the acetylenic moiety viz., the {Ac}C–H stretch, C≡C stretch and C≡C-H bends (both in-plane and out-of-plane) the *ab-initio* anharmonic calculation yields the spectrum with only one band (Figure S1, see the supporting information), which suggests that the two intense bands in the experimentally observed spectrum are not due to Fermi resonance coupling of vibrational modes localized on the acetylenic moiety. Similarly in the case of 4FPHA (Figure 2II), the IR spectrum consists of two intense bands at 3323 (**b**) and 3341 (**d**) cm^{-1} accompanied by a few weaker bands and once again the anharmonic calculation based

on the vibrational modes localized on the acetylenic group does not yield the desired spectrum (Figure S1, see the supporting information). On the other hand, fluorine substitution in the ortho and meta positions in the case of 2FPHA and 3FPHA leads to changes in the symmetry (C_s), thereby resulting in only one strong band accompanied by a few weaker bands was observed. However, even in this case, the anharmonic coupling of four vibrational modes localized on the acetylenic moiety does not yield the desired spectral pattern (Figure S1, see the supporting information). In order to faithfully capture the details of the experimentally observed spectra, several other additional ring- based normal modes which also involve displacements on the acetylenic group (Table S1 and Figures S2-S5, see the supporting information) were considered leading to an 11-D
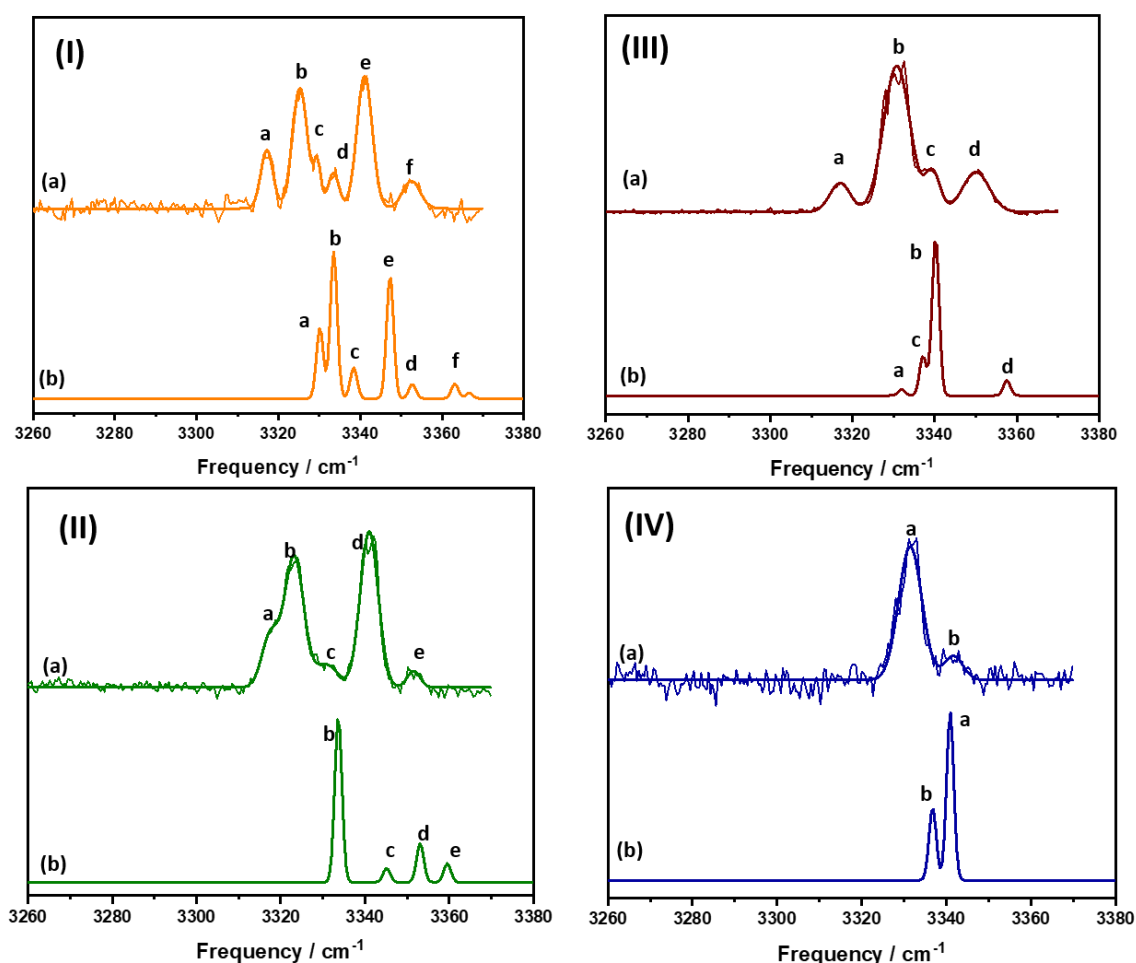

Figure 2. FDIR and simulated IR spectra of (I) PHA, (II) 4FPHA, (III) 2FPHA and (IV) 3FPHA in the {Ac}C–H stretching region. In each panel, traces (a) and (b) represent experimental and simulated spectra, respectively. The experimental spectra were fitted to the Gaussian line shape function to yield peak positions. All the simulated spectra are broadened with a Gaussian function of 2 cm^{-1} FWHM centered on calculated frequencies.

simulation, and the results are presented in Figure 2. In all four cases, the peak positions and relative intensities compare well with the corresponding experimental spectra. The comparison of the peak positions between the experimental and simulated spectra is listed in Table S2 (see the supporting information) and importantly, the maximum deviation in all the cases is less than 20 cm^{-1}. Table 1 lists all the prominent peaks observed in the simulated spectra in the {Ac}C–H stretching for PHA along with their corresponding intensities and projections over the eleven normal modes contributing to over 80% of the individual peak intensities. In the case of PHA, the band '**b**' and '**e**' at 3333 and 3347 cm^{-1}, respectively, correspond to the most intense transitions at 3325 and 3341 cm^{-1} in the experimental spectrum, show the major contributions from the {Ac}C–H stretching mode (ν_{36}) along with the combination band arising out of one quantum of C≡C

TABLE 1: List of all the prominent peak positions (cm^{-1}) observed in the simulated {Ac}C–H stretching region of PHA with their intensity (km mol^{-1}) and projections (%) over the fundamental, overtones and combination bands contributing about 80% of individual peak intensity.

Band →	3330 (a)	3333 (b)	3338 (c)	3347 (d)	3352 (e)	3363 (f)
Intensity →	11.6	24.1	5.1	20.4	2.4	2.4
Mode ↓			Projections			
ν_{36}	17.1	32.6	7.4	24.2	0.0	3.2
ν_{30}	0.0	0.0	0.0	0.0	0.0	0.0
ν_{10}	0.0	0.0	0.0	0.0	0.0	0.0
ν_{8}	0.0	0.0	0.0	0.0	0.0	0.0
$\nu_{22} + \nu_{30}$	56.8	21.5	13.9	0.0	0.0	0.0
$\nu_{23} + \nu_{30}$	17.8	4.4	15.6	49.2	0.0	0.0
$\nu_{7} + \nu_{8} + \nu_{30}$	0.0	21.7	28.1	0.0	13.35	0.0
$\nu_{6} + \nu_{10} + \nu_{30}$	0.0	0.0	0.0	0.0	0.0	50.0
$\nu_{7} + \nu_{8} + \nu_{13} + \nu_{22}$	0.0	3.0	12.11	8.8	68.1	0.0
$\nu_{7} + \nu_{8} + \nu_{13} + \nu_{23}$	0.0	7.4	15.7	0.0	5.5	0.0
$\nu_{6} + \nu_{10} + \nu_{13} + \nu_{22}$	0.0	0.0	0.0	0.0	0.0	12.7
$\nu_{6} + \nu_{10} + \nu_{13} + \nu_{23}$	0.0	0.0	0.0	0.0	0.0	25.1
$2\nu_{8} + \nu_{13} + \nu_{22}$	0.0	0.0	0.0	0.0	3.2	0.0

stretch (ν_{30}) and one quantum of ring modes ν_{22} and ν_{23}. In addition, band '**b**' also shows some contribution from a combination band that involves one quantum of C≡C–H out-of-plane bend (ν_8) along with one quantum of ring modes ν_7 and ν_{30}. Further, the weaker transitions observed in the spectrum typically comprise of combination bands that are predominantly contributed by the ring modes, in addition to the C≡C stretching mode, and marginal contribution from the C≡C–H bending modes. Similar observation can be made for the IR spectrum of 4FPHA in the {Ac}C–H stretching region (see Table S3 for projections). In the case of 2FPHA and 3FPHA, wherein only one intense peak was observed in the experimental spectra (see Figure 2), which is indicative of lowering of Fermi resonance coupling, the simulated spectra reveal maximum contribution from the {Ac}C–H mode (ν_{36}), followed by a combination band comprising of one quantum of C≡C stretch (ν_{31}) and the ring modes (ν_{22} and ν_{23}) (see Tables S4 and S5 for the projections; supporting information). On the other hand, the weaker transitions identified in the spectra can be reproduced with the involvement of C≡C-H bending motions. Thus, the above results indicate the significant contribution of the aromatic ring modes that have displacement along the acetylenic group to reproduce the observed spectral features. The agreement between the simulated and experimental spectra indicates the present set of results are in contrast with the earlier reports that the Fermi resonance coupling of modes localized on the acetylenic moiety,[6,7] but due to extensive vibrational coupling between the aromatic ring modes other than the modes localized on the acetylenic group results in the complex spectral pattern in {Ac}C–H stretching region of phenylacetylene and fluorophenylacetylenes.

The IR spectra in the aromatic C–H stretching region were also recorded and are presented in Figure 3. The FDIR spectrum of PHA in {Ar}C–H stretching region (see Figure 3I) consists of several bands in the 3020 - 3120 cm^{-1} region and cannot be solely assigned to fundamental modes of the five aromatic CH oscillators. This complex spectral feature of PHA is attributed to anharmonic coupling of aromatic C–H fundamentals with other overtones and/or combination bands, similar to the other substituted benzene derivatives.[28,34,35] The IR spectra of 2FPHA, 3FPHA, and 4FPHA in the {Ar}C–H stretching region also show several bands, similar to PHA. The IR spectra of phenylacetylene and fluorophenylacetylenes in the {Ar}C–H stretching region were computed considering all
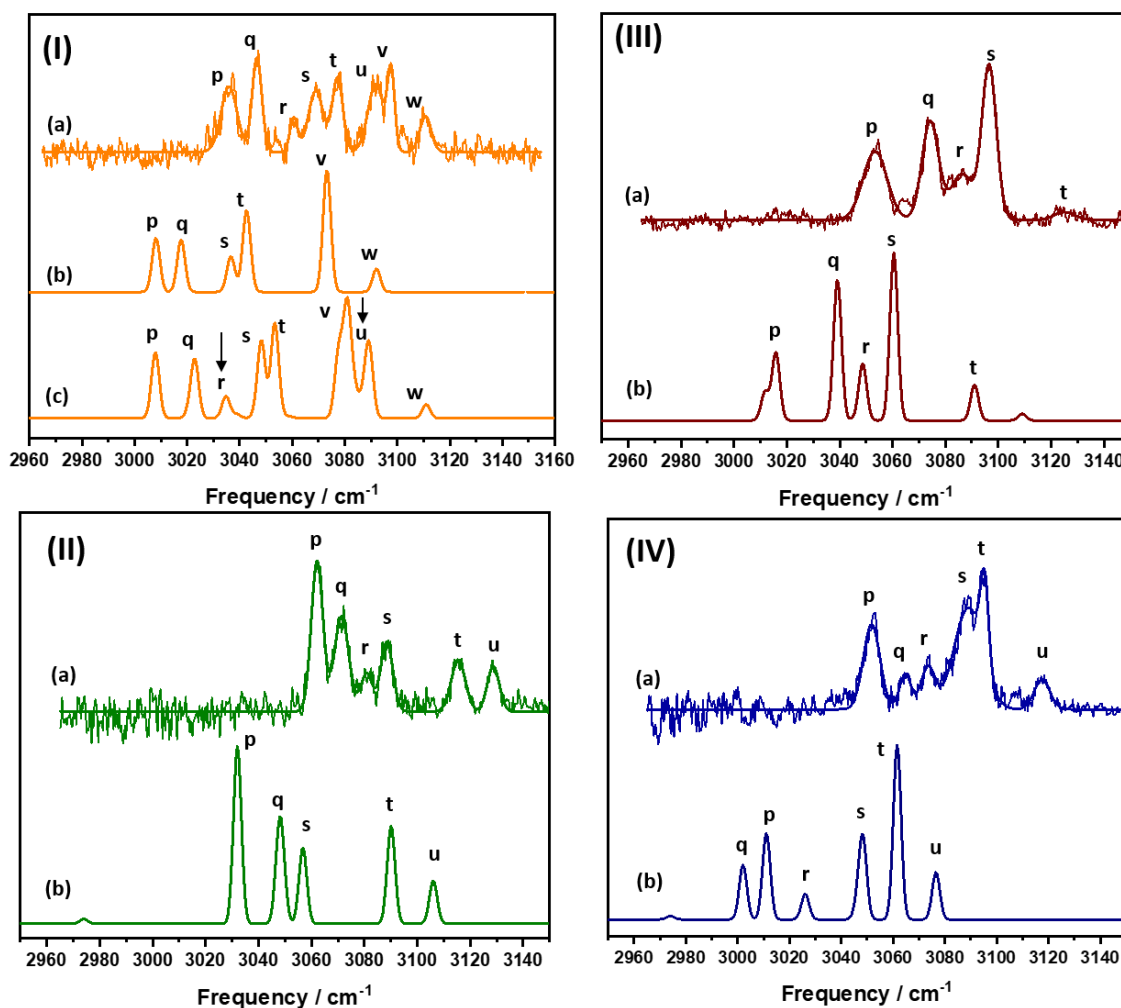
Figure 3. FDIR and simulated IR spectra of (I) PHA, (II) 4FPHA, (III) 2FPHA and (IV) 3FPHA in the acetylenic C–H stretching region. In each panel, traces (a) and (b) represent experimental and simulated spectra, respectively. The experimental spectra were fitted to the Gaussian line shape function to yield peak positions. The trace (b), in all four panels. is broadened with a Gaussian function of 2 cm^{-1} FWHM centered on calculated frequencies.

the aromatic C–H stretching modes along with the C–C stretching modes and in-plane aromatic C–H and bending modes greater than 1000 cm^{-1} (see Table S6 and the Figures S6-S9, supporting information), depicted in Figure 3, illustrates, in general, excellent agreement between the experimental and simulated spectra. However, in the case of PHA few bands are missing when the C–H bending modes greater with frequencies greater than 1000 cm^{-1} were considered. Therefore, five more in-plane bending modes (Figure S10, see the supporting information) were incorporated in the anharmonic calculations and the resulting spectrum, also depicted in Figure 3, shows a marked improvement. These results suggest that the complex spectral characteristics exhibited by PHA,

particularly in the {Ar}C–H stretching region, can be attributed to the involvement of high quanta states of lower frequency modes. The comparison of the peak positions between the experimental and simulated spectra is listed in Table S7 (see the supporting information) and for the {Ar}C–H spectra the deviations are relatively larger up to 50 cm^{-1}. Additionally, Tables S8-S11 (see the supporting information) list all the prominent peaks observed in the simulated spectra in the {Ar}C–H stretching for the four molecules considered in the present work along with their corresponding intensities and projections over all the normal modes contributing to over 80% of the individual peak intensities. The projections listed in Tables S8-S11 reveal that the prominent peaks observed in the {Ar}C–H stretching region for all the four molecules contain substantial contributions from {Ar}C–H stretching fundamental with overtones and/or combination bands that originate arising out of two quanta of aromatic C–C stretching modes and/or in-plane aromatic C–H bending modes. These observations are in accord with the earlier findings based on anharmonic couplings of aromatic C–H modes in other aromatic molecules.[28,32,34,36]

CONCLUSIONS

The observed vibrational spectra of phenylacetylene and fluorophenylacetylene in the acetylenic and aromatic C–H stretching regions were analyzed using *ab-initio* anharmonic calculations using the QP-VCI method. The IR spectrum of phenylacetylene in the acetylenic C–H stretching region shows two intense bands which have been attributed to be arising out of Fermi resonance coupling involving mode localized on the acetylenic moiety viz., the acetylenic C–H stretch, the C≡C stretch and C≡C–H out-of-plane bend. However, spectral simulation reveals that several ring modes that involve C–C≡C displacements are vital and must be included to reproduce all the features of the experimentally observed spectra. These results are in contrast to the earlier reports and indicate the delocalization of vibrational coupling to the aromatic ring in the case of {Ac}C–H stretching region. Further, the complex spectral features observed in the case of {Ar}C–H stretching region were captured with the inclusion of multiple aromatic C–H stretching and bending modes along with the aromatic C–C stretching mode in the spectral simulation. The results indicate that the anharmonic coupling among the bending and stretching motions of {Ar}C–H oscillators is responsible for the complex

spectral feature, similar to the other aromatic molecules. The reasonable agreement of the simulated spectra with the observed spectral features in both cases validates the reliability of the QP-VCI method in capturing the anharmonic coupling of complex molecular systems.

REFERENCES

1   G. C. Pimentel and A. L. McClellan, *The Hydrogen Bond*, W. H. Freeman and Company, San Francisco, 1960.

2   G. A. Jaffery, *An Introduction to Hydrogen Bonding*, Oxford University Press, New York, 1997.

3   G. N. Patwari and J. M. Lisy, Cyclohexane as a Li+ Selective Ionophore, *J Phys Chem A*, 2007, **111**, 7585–7588.

4   M. N. Slipchenko, B. G. Sartakov, A. F. Vilesov and S. S. Xantheas, Study of NH stretching vibrations in small ammonia clusters by infrared spectroscopy in he droplets and ab initio calculations, *J. Phys. Chem. A*, 2007, **111**, 7460–7471.

5   R. A. Nyquist and W. J. Potts, Infrared absorptions characteristic of the terminal acetylenic group, *Spectrochim. Acta*, 1960, **16**, 419–427.

6   G. W. King and S. P. So, Ethynylbenzene; The vibrational spectra of some deuterated isomers, *J. Mol. Spectrosc.*, 1970, **36**, 468–487.

7   J. A. Stearns and T. S. Zwier, Infrared and ultraviolet spectroscopy of jet-cooled ortho-, meta-, and para-diethynylbenzene, *J. Phys. Chem. A*, 2003, **107**, 10717–10724.

8   P. C. Singh, B. Bandyopadhyay and G. N. Patwari, Structure of the phenylacetylene - Water complex as revealed by infrared-ultraviolet double resonance spectroscopy, *J. Phys. Chem. A*, 2008, **112**, 3360–3363.

9   S. Maity, M. Guin, P. C. Singh and G. N. Patwari, Phenylacetylene: A hydrogen bonding chameleon, *ChemPhysChem*, 2011, **12**, 26–46.

10 S. Maity and G. N. Patwari, Hydrogen Bonding to Multifunctional Molecules:

Spectroscopic and ab Initio Investigation of Water Complexes of Fluorophenylacetylenes, *J. Phys. Chem. A*, 2009, **113**, 1760–1769.

11 A. Dey, S. I. Mondal, S. Sen and G. N. Patwari, Spectroscopic and Ab Initio Investigation of C-H..N Hydrogen-Bonded Complexes of Fluorophenylacetylenes: Frequency Shifts and Correlations, *ChemPhysChem*, 2016, **17**, 2509–2515.

12 S. Mishra, D. K. Sahoo, P. J. Hsu, Y. Matsuda, J. L. Kuo, H. S. Biswal and G. N. Patwari, A liquid crucible model for aggregation of phenylacetylene in the gas phase, *Phys. Chem. Chem. Phys.*, 2019, **21**, 13623–13632.

13 S. Singh, P.-J. Hsu, J.-L. Kuo and G. N. Patwari, Dipole moment enhanced π–π stacking in fluorophenylacetylenes is carried over from gas-phase dimers to crystal structures propagated through liquid like clusters, *Phys. Chem. Chem. Phys.*, 2021, **23**, 9938–9947.

14 Q. R. Huang, T. Endo, S. Mishra, B. Zhang, L. W. Chen, A. Fujii, L. Jiang, G. N. Patwari, Y. Matsuda and J. L. Kuo, Understanding Fermi resonances in the complex vibrational spectra of the methyl groups in methylamines, *Phys. Chem. Chem. Phys.*, 2021, **23**, 3739–3747.

15 D. M. Hewett, S. Bocklitz, D. P. Tabor, E. L. Sibert, M. A. Suhm and T. S. Zwier, Identifying the first folded alkylbenzene via ultraviolet, infrared, and Raman spectroscopy of pentylbenzene through decylbenzene, *Chem. Sci.*, 2017, **8**, 5305–5318.

16 E. G. Buchanan, J. C. Dean, T. S. Zwier and E. L. Sibert, Towards a first-principles model of Fermi resonance in the alkyl CH stretch region: Application to 1,2-diphenylethane and 2,2,2-paracyclophane, *J. Chem. Phys.*, 2013, **138**, 064308.

17 K.-L. Ho, L.-Y. Lee, M. Katada, A. Fujii and J.-L. Kuo, An ab initio anharmonic approach to study vibrational spectra of small ammonia clusters, *Phys. Chem. Chem. Phys.*, 2016, **18**, 30498–30506.

18 E. L. Sibert, D. P. Tabor, N. M. Kidwell, J. C. Dean and T. S. Zwier, Fermi resonance effects in the vibrational spectroscopy of methyl and methoxy groups, *J. Phys. Chem. A*, 2014, **118**, 11272–11281.

19 D. P. Tabor, D. M. Hewett, S. Bocklitz, J. A. Korn, A. J. Tomaine, A. K. Ghosh, T. S. Zwier and E. L. S. III, Anharmonic modeling of the conformation-specific IR spectra of ethyl, n-propyl, and n-butylbenzene, *J. Chem. Phy.*, 2016, **144**, 224310.

20 K. Yagi, S. Hirata and K. Hirao, Vibrational quasi-degenerate perturbation theory: Applications to fermi resonance in CO2, H2CO, and C6H6, *Phys. Chem. Chem. Phys.*, 2008, **10**, 1781–1788.

21 B. Thomsen, K. Yagi and O. Christiansen, A simple state-average procedure determining optimal coordinates for anharmonic vibrational calculations, *Chem. Phys. Lett.*, 2014, **610**–**611**, 288–297.

22 J. Liu, J. Yang, X. C. Zeng, S. S. Xantheas, K. Yagi and X. He, Towards complete assignment of the infrared spectrum of the protonated water cluster H+(H2O)21, *Nat. Commun.*, 2021, **12**, 6141.

23 L. Sagiv, B. Hirshberg and R. B. Gerber, Anharmonic vibrational spectroscopy calculations using the ab initio CSP method: Applications to H2CO3, (H2CO3)2, H2CO3-H2O and isotopologues, *Chem. Phys.*, 2018, **514**, 44–54.

24 B. J. Miller, L. Du, T. J. Steel, A. J. Paul, A. H. Södergren, J. R. Lane, B. R. Henry and H. G.

Kjaergaard, Absolute intensities of NH-stretching transitions in dimethylamine and pyrrole, *J. Phys. Chem. A*, 2012, **116**, 290–296.

25 H. G. Kjaergaard, A. L. Garden, G. M. Chaban, R. B. Gerber, D. A. Matthews and J. F. Stanton, Calculation of vibrational transition frequencies and intensities in water dimer: Comparison of different vibrational approaches, *J. Phys. Chem. A*, 2008, **112**, 4324–4335.

26 Q.-R. Huang, Y.-C. Li, K.-L. Ho and J.-L. Kuo, Vibrational spectra of small methylamine clusters accessed by an ab initio anharmonic approach, *Phys. Chem. Chem. Phys.*, 2018, **20**, 7653–7660.

27 S. Tanabe, T. Ebata, M. Fujii and N. Mikami, OH stretching vibrations of phenol-(H2O)n(n=1-3) complexes observed by IR-UV double-resonance spectroscopy, *Chem. Phys. Lett.*, 1993, **215**, 347–352.

28 R. H. Page, Y. R. Shen and Y. T. Lee, Infrared-ultraviolet double resonance studies of benzene molecules in a supersonic beam, *J. Chem. Phys.*, 1988, **88**, 5362–5376.

29 P. C. Singh and G. N. Patwari, Infrared-optical double resonance spectroscopy: A selective and sensitive tool to investigate structures of molecular clusters in the gas phase, *Curr. Sci.*, 2008, **95**, 469–474.

30 M. J. Frisch, G. W. Trucks, H. B. Schlegel, *et al*. G. E. Scuseria, M. A. Robb, J. R. Cheeseman, G. Scalmani, V. Barone, G. A. Petersson, H. Nakatsuji, X. Li, M. Caricato, A. V. Marenich, J. Bloino, B. G. Janesko, R. Gomperts, B. Mennucci, H. P. Hratchian, J. V. Ortiz, A. F. Izmaylov, J. L. Sonnenberg, D. Williams-Young, F. Ding, F. Lipparini, F. Egidi, J. Goings, B. Peng, A. Petrone, T. Henderson, D. Ranasinghe, V. G. Zakrzewski, J. Gao, N. Rega, G. Zheng, W. Lia. ng, M. Hada, M. Ehara, K. Toyota, R. Fukuda, J. Hasegawa, M. Ishida, T. Nakajima, Y. Honda, O. Kitao, H. Nakai, T. Vreven, K. Throssell, J. Montgomery, J. A., J. E. Peralta, F. Ogliaro, M. J. Bearpark, J. J. Heyd, E. N. Brothers, K. N. Kudin, V. N. Staroverov, T. A. Keith, R. Kobayashi, J. Normand, K. Raghavachari, A. P. Rendell, J. C. Burant, S. S. Iyengar, J. Tomasi, M. Cossi, J. M. Millam, M. Klene, C. Adamo, R. Cammi, J. W. Ochterski, R. L. Martin, K. Morokuma, O. Farkas, J. B. Foresman and D. J. Fox, Gaussian-16, Rev.B01, Gaussian Inc, Wallingford CT, 2016.

31 V. Barone, Anharmonic vibrational properties by a fully automated second-order perturbative approach, *J. Chem. Phys.*, 2005, **122**, 014108.

32 J. Y. Feng, Q. R. Huang, H. Q. Nguyen, J. L. Kuo and T. Ebata, Infrared–vacuum ultraviolet spectroscopy of the C-H stretching vibrations of jet-cooled aromatic azine molecules and the anharmonic analysis, *J. Chinese Chem. Soc.*, 2022, **69**, 160–172.

33 J. A. Stearns and T. S. Zwier, Infrared and ultraviolet spectroscopy of jet-cooled ortho-, meta-, and para-diethynylbenzene, *J. Phys. Chem. A*, 2003, **107**, 10717–10724.

34 C. Minejima, T. Ebata and N. Mikami, C-H stretching vibrations of benzene and toluene in their S1 states observed by double resonance vibrational spectroscopy in supersonic jets, *Phys. Chem. Chem. Phys.*, 2002, **4**, 1537–1541.

35 T. Watanabe, T. Ebata, S. Tanabe and N. Mikami, Size-selected vibrational spectra of phenol-(H2O)n (n=1–4) clusters observed by IR–UV double resonance and stimulated Raman-UV double resonance spectroscopies, *J. Chem. Phy.*, 1996, **105**, 408–419.

36 J. Feng, Y. Lee, C. Zhu, P. Hsu, J. Kuo and T. Ebata, IR–VUV spectroscopy of pyridine dimers, trimers and pyridine–ammonia complexes in a supersonic jet, *Phys. Chem. Chem. Phys.*, 2002, **22**, 21520–21534.